# Mechanism of Ruthenium-Catalyzed Alder Ene-Type Reaction: A Theoretical Study

Hui Chen and Shuhua Li*

*Department of Chemistry, Institute of Theoretical and Computational Chemistry, Laboratory of Mesoscopic Chemistry, Nanjing University, Nanjing 210093, People's Republic of China*

*Received August 8, 2004*

Density functional calculations have been used to explore the potential energy profiles of the Alder ene reaction catalyzed by CpRu(COD)Cl in polar solvents. Three model catalysts, CpRuCl, $CpRu(H_2O)^+$, and $CpRu^+$, have been investigated separately, and the results are compared. Our calculations reveal that with CpRuCl as the catalyst the ruthenacyclopentene mechanism is clearly preferred over the $\pi$-allylruthenium mechanism. The rate-determining step is the oxidative coupling of the coordinated alkyne and alkene groups to form a ruthenacyclopentene intermediate, which has a free energy barrier of 14.2 kcal/mol in the methanol solvent. When $CpRu(H_2O)^+$ or $CpRu^+$ is assumed to be the operative catalyst, both the ruthenacyclopentene mechanism and the $\pi$-allylruthenium mechanism are found to be comparable in their energetics, and it is hard to determine which pathway is more favorable from the present calculations. The results obtained with CpRuCl as the catalyst are in good agreement with the related experimental facts.

## Introduction

Carbon−carbon bond formation is one of the main aspects of organic chemistry. In recent years, ruthenium-catalyzed carbon−carbon bond formation reactions have received a great deal of attention.[1−7] The Alder ene reaction, as shown in Scheme 1, provides an atom-economical process for C−C bond formation.

**Scheme 1**

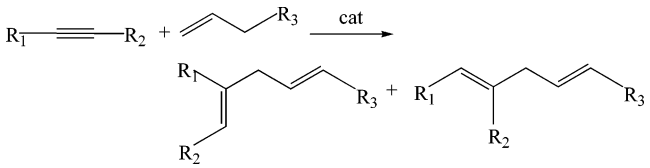


Without efficient catalysts, this reaction frequently requires extreme conditions and exhibits a lack of selectivity.[8] Trost et al. found that some ruthenium complexes can catalyze this reaction efficiently, and the catalyzed reactions exhibit high chemoselectivity and regioselectivity.[6] This catalyzed reaction has had many useful applications, such as the synthesis of 1,1-disubstituted alkenes,[12] trisubstituted alkenes,[14] alternaric acid,[15] amphidinolide A,[9] and ancepsenolide.[16] The ruthenium catalysts for this reaction include complexes such as CpRu(COD)Cl, $CpRu(CH_3CN)_3PF_6$,[10,11] and Cp*Ru(COD)Cl and some other structurally similar complexes. The reaction often occurs in polar solvents such as methanol, DMF−$H_2O$, DMF, and acetone and often needs only reflux in the solvent or even takes place at room temperature. Functional groups such as hydroxyl groups, ketones, and ester either in the alkyne or in the alkene can undergo this reaction without deleterious effects.

The understanding of the mechanism of this ruthenium-catalyzed Alder ene reaction has changed a great deal since the discovery of the reaction. At first, the reaction was thought to go through a $\pi$-allylruthenium intermediate. Later, however, experimental results showed that the reaction might proceed via a ruthenacyclopentene intermediate.[6] The proposed ruthenacyclopentene and $\pi$-allylruthenium mechanisms are shown in Schemes 2 and 3, respectively.

Although the above ruthenacyclopentene mechanism has been successfully used to explain some of the substituent effects observed experimentally, theoretical

(1) Trost, B. M.; Toste, F. D.; Pinkerton, A. B. *Chem. Rev.* **2001**, *101*, 2067.
(2) (a) Chatani, N.; Kataoka, K.; Murai, S.; Seki, Y. Furukawa, N. *J. Am. Chem. Soc.* **1998**, *120*, 9104. (b) Noels, A. F.; Demonceau, A.; Carlier, E.; Hubert, A. J.; Marquez-Silva, R. L.; Sanchez-Delgado, R. A. *J. Chem. Soc., Chem. Commun.* **1988**, 783. (c) Demonceau, A.; Abreu Dias, E.; Lemoine, C. A.; Stumpf, A. W.; Noels, A. F. *Tetrahedron Lett.* **1995**, *36*, 3519.
(3) (a) Trost, B. M.; Toste, F. D.; Shen, H. *J. Am. Chem. Soc.* **2000**, *122*, 2379. (b) Trost, B. M.; Shen, H. *Org. Lett.* **2000**, *2*, 2523.
(4) Jordan, R. W.; Tam, W. *Org. Lett.* **2001**, *3*, 2367.
(5) Yamamoto, Y.; Kitahara, H.; Hattori, R.; Itoh, K. *Organometallics* **1998**, *17*, 910.
(6) (a) Trost, B. M.; Indolese, A. *J. Am. Chem. Soc.* **1993**, *115*, 4361. (b) Trost, B. M.; Indolese, A. F.; Müller, T. J. J.; Treptow, B. *J. Am. Chem. Soc.* **1995**, *117*, 615.
(7) Morusaki, Y.; Kondo, T.; Mitsudo, T. *Organometallics* **1999**, *18*, 4742.
(8) Snider, B. B. *Acc. Chem. Res.* **1980**, *13*, 426.
(9) Trost, B. M.; Roth, G. J. *Org. Lett.* **1999**, *1*, 67.
(10) Albers, M. O.; Robinson, D. J.; Shaver, A.; Singleton, E. *Organometallics* **1986**, *5*, 2199.
(11) Gill. T. P.; Mann. K. R. *Organometallics* **1982**, *1*, 485.
(12) Trost, B. M.; Pinkerton, A. B.; Toste, F. D.; Sperrle, M. *J. Am. Chem. Soc.* **2001**, *123*, 12504.
(13) Trost, B. M.; Imi, K.; Indoleses, A. *J. Am. Chem. Soc.* **1993**, *115*, 8831.
(14) Trost, B. M.; Shen, H.; Pinkerton, A. B. *Chem. Eur. J.* **2002**, *8*, 2341.
(15) Trost, B. M.; Probst, G. D.; Schoop, A. *J. Am. Chem. Soc.* **1998**, *120*, 9228.
(16) (a) Barry, B. M.; Müller, T. J. J. *J. Am. Chem. Soc.* **1994**, *116*, 4985. (b) Barry, B. M.; Müller, T. J. J.; Matinez, J. *J. Am. Chem. Soc.* **1995**, *117*, 1888.

10.1021/om049384i CCC: $30.25 
Publication on Web 02/04/2005

**Scheme 2**

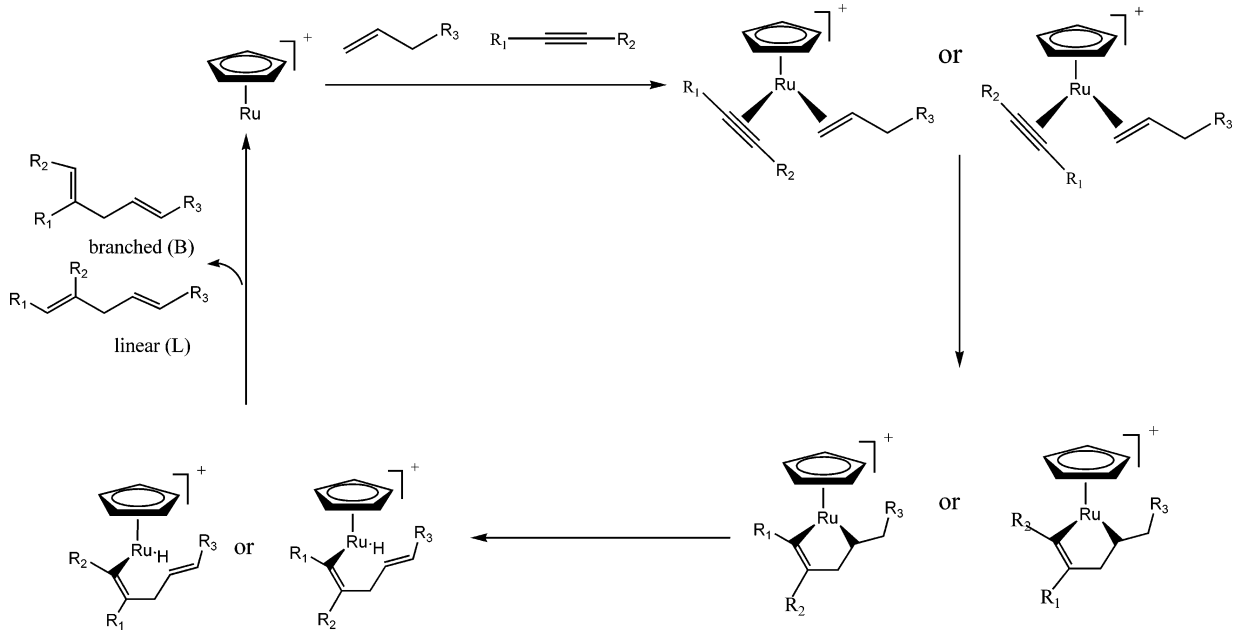


**Scheme 3**

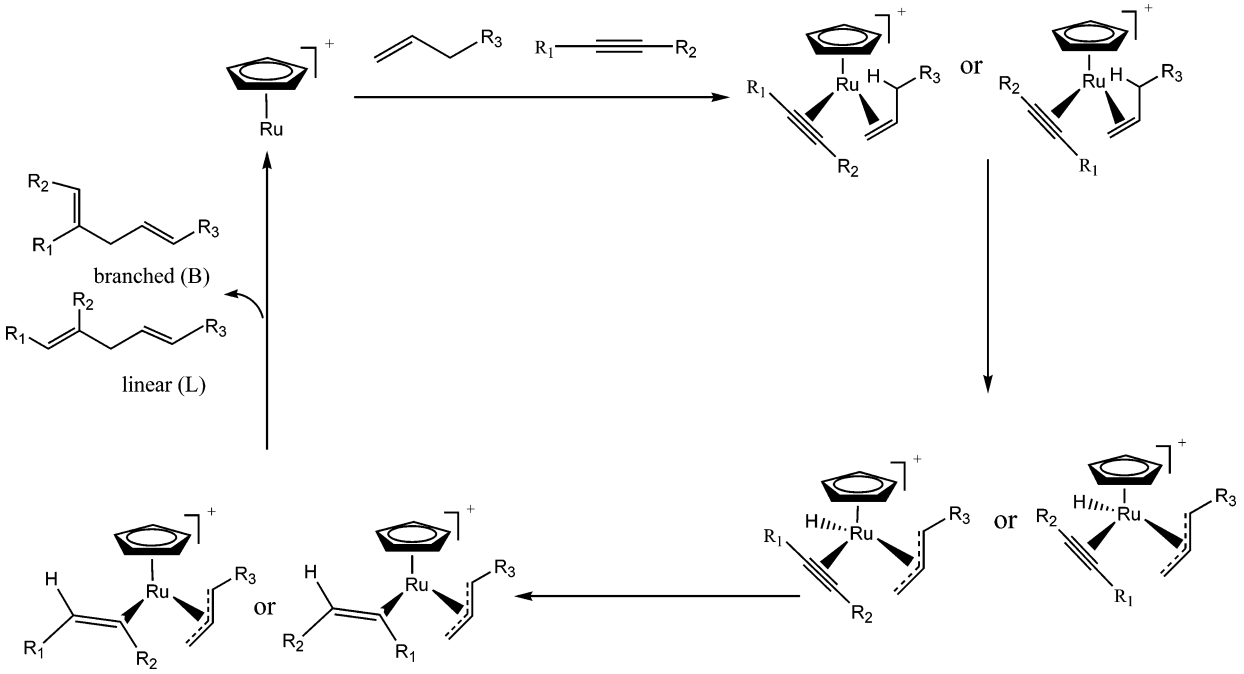


investigations of both of these mechanisms of this reaction are desirable, for a more comprehensive understanding.

In this paper, our aim is to theoretically study the potential energy profiles of the Alder ene reaction catalyzed by CpRu(COD)Cl in polar solvents to gain a general understanding of the mechanism of this type of reaction. A model reaction with $R_1 = H$, $R_2 = H$, and $R_3 = H$ as in Scheme 1 has been employed, and the three model catalysts CpRuCl, $CpRu(H_2O)^+$, and $CpRu^+$ have been investigated separately. For each model catalyst, the potential energy profiles of the reaction within the $\pi$-allylruthenium and ruthenacyclopentene mechanisms will be fully explored and compared. Then the most possible reaction mechanism for each model catalyst is proposed. The results of this study might be useful to experimentalists for inventing more effective catalysts for similar Alder ene-type reactions.

## Methodology and Computational Details

Stationary points on the potential energy surfaces are calculated with the Gaussian98 package.[17] Density functional theory is employed with the three-parameter hybrid exchange functional of Becke and the Lee, Yang, and Parr correlation functional (B3LYP).[18−20] For ruthenium, relativistic effective core potential (ECP)[21] is employed in all B3LYP calculations. The basis set for Ru is a modified LANL2DZ double-$\zeta$ basis set plus an f-type polarization function,[22] in which the two 5p functions of the standard LANL2DZ have been replaced by the optimized 5p functions from Couty and Hall.[23] For all the other atoms, the 6-31G(d,p) basis set is employed for all geometry optimizations. Full geometry optimizations have

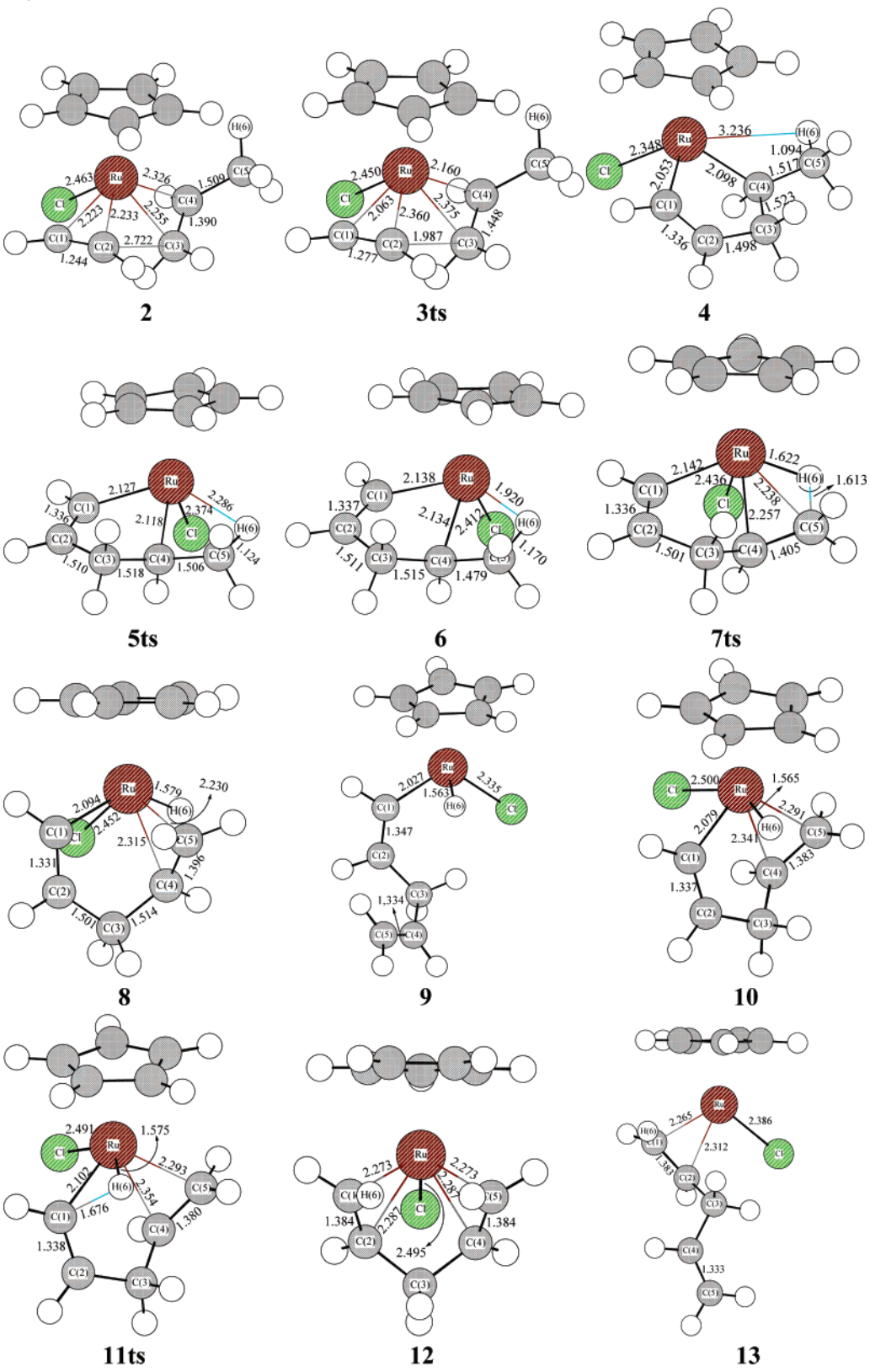


been performed to obtain the structures of reactants, intermediates, transition states, and products. For each species, a frequency calculation is done to calculate zero-point energies (ZPE) and to verify whether it is a minimum or a transition state. Then the enthalpies and Gibbs free energies of the stationary points are calculated at the temperature of 298 K. To consider the bulk solvent effects on the energetics of each species, we use the polarizable-continuum model (PCM)[24] with methanol as the solvent to calculate the Gibbs free energy of solvation for each species using its gas-phase optimized geometry. The free energy for each species in solution is taken as the sum of the gas-phase free energy and the free energy of solvation.

## Results and Discussion

We have employed three model catalysts in our calculations, CpRuCl (model I), $CpRu(H_2O)^+$ (model II),

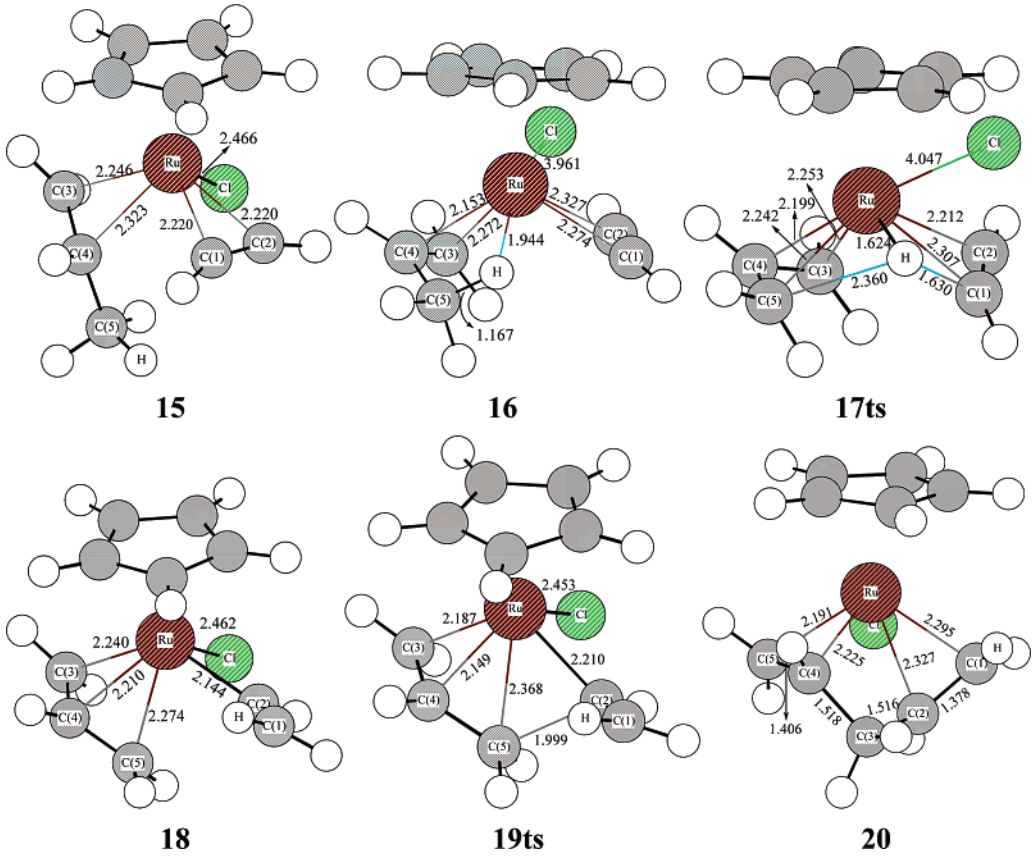


**Figure 1.** B3LYP-optimized structures of **2**−**20** obtained with model I.

and $CpRu^+$ (model III). Model I comes from the experimental catalyst CpRu(COD)Cl by releasing the labile COD ligand. Since in a polar solvent the chloride is possibly replaced by a solvent molecule, as shown by

$$CpRuCl + L\,(solvent) \rightarrow CpRuL^+ + Cl^- \qquad (1)$$

the catalyst may also exist in the form $Cp(Ru)L^+$. For simplicity here we choose L= $H_2O$ in model II. This viewpoint is supported by the experimental fact that a large excess of chloride, which would shift the above substitution reaction to the neutral complex, indeed slowed the reaction in methanol.[6b] Another form of the catalyst is the uncoordinated complex $CpRu^+$ (model III), which may occur in the dissociation reaction

$$CpRuCl + L\,(solvent) \rightarrow CpRu^+ + Cl^- + L \qquad (2)$$

It is valuable to compare the Gibbs free energy changes for the substitution reaction and the dissociation reaction mentioned above in the solvent methanol. Our calculations with the PCM method show that the free energy changes are 10.1 and 20.5 kcal/mol for reactions 1 and 2, respectively. In addition, the electronic energy barrier for the dissociation of the chloride ligand from CpRuCl is estimated to be more than 25.0 kcal/mol in methanol. These results imply that in a polar solvent such as methanol the working catalyst may mainly exist in the form of model I, whereas models II and III are the less probable catalysts. However, the use of different polar solvents may have a significant effect on the position of the substitution or dissociation reaction described above. Therefore, the title reaction catalyzed by three model catalysts have been investigated and compared for general purposes. Two of the most possible reaction mechanisms, the ruthenacyclopentene mechanism and the $\pi$-allylruthenium mechanism, have been explored separately for each reaction.

(17) Frisch, M. J.; Trucks, G. W.; Schlegel, H. B.; Scuseria, G. E.; Robb, M. A.; Cheeseman, J. R.; Zakrzewski, V. G.; Montgomery, J. A., Jr.; Stratmann, R. E.; Burant, J. C.; Dapprich, S.; Millam, J. M.; Daniels, A. D.; Kudin, K. N.; Strain, M. C.; Farkas, O.; Tomasi, J.; Barone, V.; Cossi, M.; Cammi, R.; Mennucci, B.; Pomelli, C.; Adamo, C.; Clifford, S.; Ochterski, J.; Petersson, G. A.; Ayala, P. Y.; Cui, Q.; Morokuma, K.; Malick, D. K.; Rabuck, A. D.; Raghavachari, K.; Foresman, J. B.; Cioslowski, J.; Ortiz, J. V.; Baboul, A. G.; Stefanov, B. B.; Liu, G.; Liashenko, A.; Piskorz, P.; Komaromi, I.; Gomperts, R.; Martin, R. L.; Fox, D. J.; Keith, T.; Al-Laham, M. A.; Peng, C. Y.; Nanayakkara, A.; Challacombe, M.; Gill, P. M. W.; Johnson, B.; Chen, W.; Wong, M. W.; Andres, J. L.; Gonzalez, C.; Head-Gordon, M.; Replogle, E. S.; Pople, J. A. *Gaussian 98*, Revision A.9; Gaussian, Inc., Pittsburgh, PA, 1998.

(18) (a) Beck, A. D. *J. Chem. Phys.* **1993**, *98*, 5648. (b) Lee, C.; Yang, W.; Parr, R. *Phys. Rev. B* **1988**, *37*, 785.

(19) For reviews of density functional theories, see: (a) Parr, R. G.; Yang, W. *Density Functional Theory of Atoms and Molecules*; Oxford University Press: New York, 1989. (b) Ziegler, T. *Chem. Rev*. **1991**, *91*, 651. (c) *Density Functional Methods in Chemistry*; Labanowski, J., Andzelm, J., Eds.; Springer: Berlin, 1991.

(20) B3LYP calculations give relative energies of the various structural transition-metal intermediates to be within ~5 kcal/mol of the actual energies: (a) Dunietz, B. D.; Beachy, M. D.; Cao, Y.; Whittington, D. A.; Lippard, S. J.; Friesner, R. A. *J. Am. Chem. Soc.* **2000**, *122*, 2828. (b) Ricca, A.; Bauschlicher, C. W. *Theor. Chim. Acta* **1995**, *92*, 123. (c) Ricca, A.; Bauschlicher, C. W. *J. Phys. Chem*. **1995**, *99*, 5922. (d) Ricca, A.; Bauschlicher, C. W. *J. Phys. Chem.* **1997**, *101*, 8949. (e) Glukhovstev, M. N.; Bach, R. D.; Nagel, C. J. *J. Phys. Chem.* **1997**, *101*, 316. (f) Blomberg, M. R. A.; Siegbahn, P. E. M.; Svensson, M. *J. Chem. Phys.* **1996**, *104*, 9546.

(21) Hay, P. J.; Wadt, W. R. *J. Chem. Phys.* **1985**, *82*, 299.

(22) Ehler, A. W.; Böhme, M.; Dapprich, S.; Gobbi, A.; Höllwarth, A.; Jonas, V.; Köhler, K. F.; Stegmann, R.; Velkamp, A.; Frenking, G. *Chem. Phys. Lett.* **1993**, *208*, 111.

(23) Couty, M.; Hall, M. B. *J. Comput. Chem.* **1996**, *17*, 1359.

(24) Tomasi, J.; Persico, M. *Chem. Rev*. **1994**, *94*, 2027.

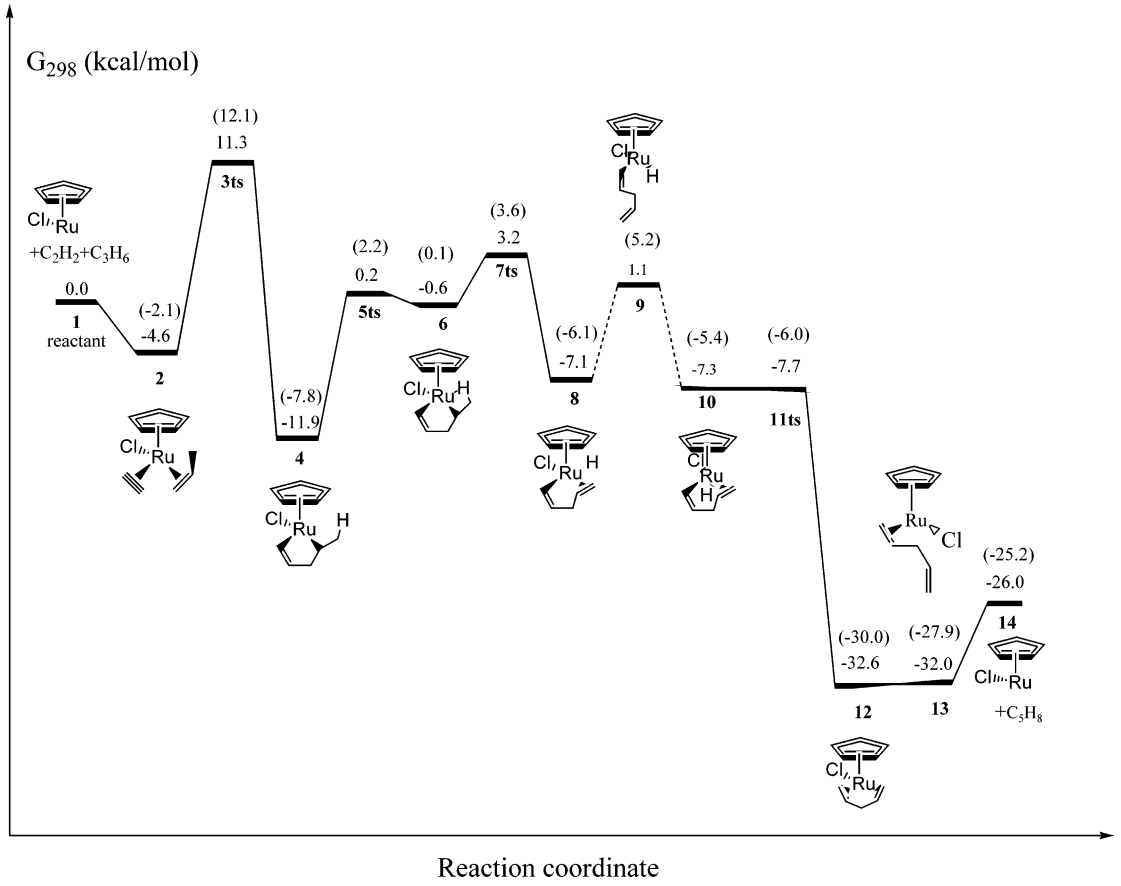


**Figure 2.** Free energy profile of the ruthenacyclopentene mechanism with model I in the gas phase and in the solution phase (values in parentheses).

For each model catalyst, the relative electronic energies and Gibbs free energies of all the stationary points in the gas phase and in the solution phase are given in the Supporting Information.

**CpRuCl.** First, we will investigate the ruthenacyclopentene mechanism. With this model catalyst, the optimized geometries are shown in Figure 1, and the free energy profile of this reaction in the gas phase and in the solution phase is given in Figure 2. Initially, the reactants, propene and ethyne, are $\pi$-coordinated to the catalyst **1** to yield the encounter complex **2**. Then propene and ethyne couple to produce the ruthenacyclopentene intermediate **4** through the transition state **3ts**. The free energy barrier of this oxidative coupling step is 15.9 kcal/mol. Next, the agostic intermediate **6** is formed through the transition state **5ts**. The subsequent $\beta$-H elimination produces the Ru(IV) hydride intermediate **8**. The free energy barrier of this $\beta$-H elimination step is only 3.8 kcal/mol. Then the coordinated $C_4-C_5$ double bond dissociates from the Ru atom to form **9** so that the hydride atom can move to the cis position of the $Ru-C_1$ bond. It is difficult to capture the transition state for the dissociation step of the double bond, but the energy barrier should be close to the dissociation energy, which is 8.2 kcal/mol. Then, the $C_4-C_5$ double bond in **9** may recoordinate to the metal to form another hydride intermediate **10**, which is almost isoenergetic with the hydride intermediate **8**. Now the hydride intermediate **10** is able to undergo a reductive elimination through the transition state **11ts** to produce the intermediate **12** with the 1,4-diene $\pi$-coordinated to the metal. This reductive elimination step is barrierless when the free energy of the transition state is compared to that of the reactant. By dissociation of one metal−alkene bond, the species **12** can be easily converted into **13**. Finally, the product, 1,4-diene, can be released from the species **13**, and the catalyst is regenerated. To conclude, since the free energy of the transition state **3ts** is the highest among all the species, the C−C coupling process should be the rate-limiting step in the ruthenacyclopentene mechanism. The overall exothermicity of the studied reaction in methanol is about 25.2 kcal/mol.

Now let us turn to the $\pi$-allylruthenium mechanism. The free energy profile of this mechanism is shown in Figure 3, and the corresponding optimized structures are collected in Figure 1. Along this reaction path, the first step is also the formation of the encounter complex **15**. After this step, one C−H bond in the methyl group of the propene ligand approaches the metal to form the $\beta$-H agostic intermediate **16**. We failed to locate the transition state connecting **15** and **16**, probably because in the transition state the Ru−Cl bond must be significantly stretched simultaneously to make a vacant coordination site on the metal available for the approaching $\beta$-H, as seen from the structure of **16**. However, the agostic complex **16** is 30.9 kcal/mol higher in free energy than the complex **15**, implying that the formation of **16** is very difficult. If the reaction proceeds, the next step is the transfer of the $\beta$-H from the methyl group of the propene ligand to the ethyne ligand to form the $\pi$-allylruthenium complex **18**. Interestingly, $\beta$-H elimination does not occur, because the resultant hydride complex is not a minimum on the potential energy

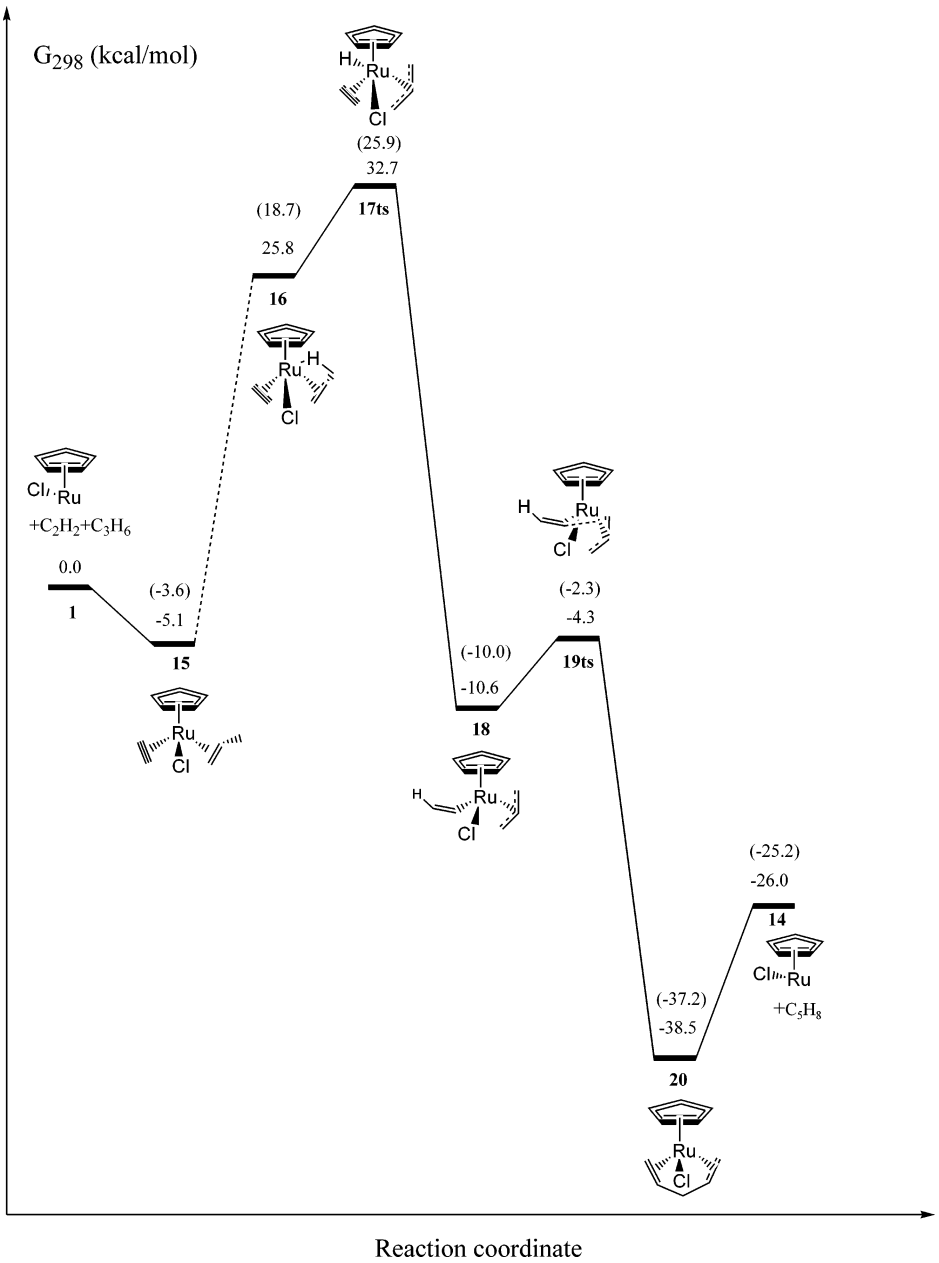


**Figure 3.** Free energy profile of the $\pi$-allylruthenium mechanism with model I in the gas phase and in the solution phase (values in parentheses).

surface. The free energy barrier from **16** to **18** is 6.9 kcal/mol. Then, the allyl ligand and the vinyl ligand reductively couple to form the 1,4-diene complex **20**, through the transition state **19ts** with a barrier of 6.3 kcal/mol. This reductive coupling step is strongly exothermic by about 28 kcal/mol. Finally, the loss of the 1,4-diene product from **20** may be facile, and the catalyst can be regenerated. In summary, the highest point on the potential energy surface is **17ts**, which is 32.7 kcal/mol above the reactants.

Up to now, we have not taken into account the bulk solvent effect on the free energy profiles within both reaction mechanisms. Using the PCM method with methanol as the solvent, the calculated free energies for all the stationary points in solution within the ruthenacyclopentene mechanism are also listed in Figure 2 for comparison. One can see that the free energy of solvation is relatively small for all species occurring in Figures 2 and 3, and the free energy profile obtained in the gas phase is not significantly changed by the bulk solvent effect. For example, the free energy barrier of the rate-limiting C−C coupling step decreases only by 1.7 kcal/mol (from 15.9 to 14.2 kcal/mol) after the solvent effect is included. In the $\pi$-allylruthenium mechanism for the rate-limiting step, the formation of the $\beta$-H agostic intermediate **16**, our calculations show that the free energy change of this step in methanol is still 22.3 kcal/mol.

By comparing the calculated free energy profiles of these two mechanisms in methanol, one can see clearly that when the catalyst predominantly exists in the form of CpRuCl the ruthenacyclopentene mechanism is much more favorable kinetically than the $\pi$-allylruthenium mechanism.

On the basis of the above discussions, it may be worthwhile to briefly discuss the optimized geometries of some key species within the ruthenacyclopentene mechanism. From the structure of the encounter com-

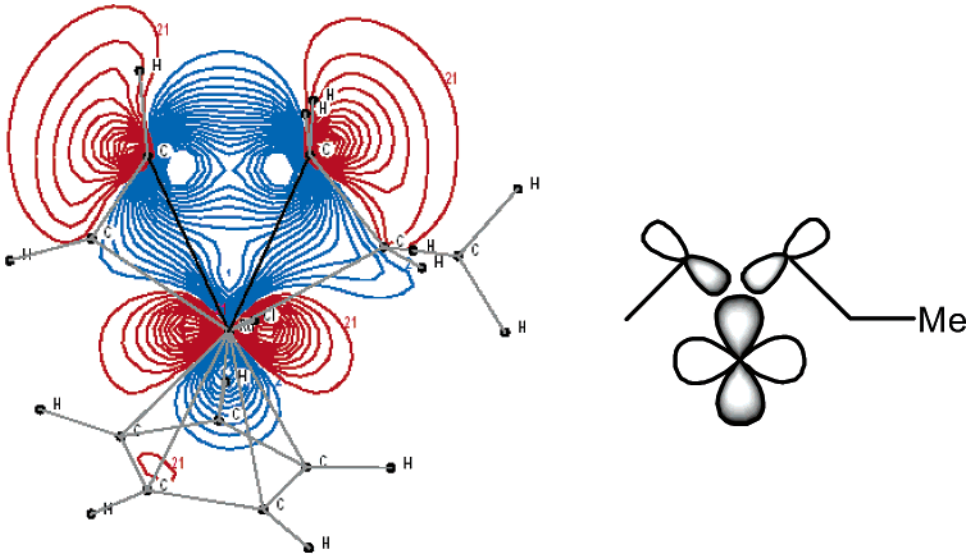


**Figure 4.** Orbital interaction between two p orbitals of $C_2$, $C_3$ and the d orbital of Ru in **3ts**.

plex **2**, one can see that the two C−C bonds of the coordinated propene and ethyne are activated to some extent, since in the isolated propene and ethyne these two bonds are 1.333 and 1.205 Å, respectively. The structure of the C−C coupling transition state **3ts** shows that this transition state is midway on the path from **2** to **4**. In **3ts**, the $C_2$−$C_3$ bond is 1.987 Å, much shorter than the 2.722 Å bond length in **2** but still considerably longer than the 1.498 Å length in **4**. Figure 4 provides a picture of the molecular orbital interaction that leads to the C−C bond formation in **3ts**. Clearly, the Ru atom plays an important role in the C−C coupling process. The intermediate **6** is a complex in which there is strong agostic interaction between the $C_5$−$H_6$ bond and the metal center, as seen from the Ru−$H_6$ and $C_5$−$H_6$ distances. The transition state **5ts** connecting **4** and **6** is a three-centered "late" transition state.

In the hydride intermediate **8**, the $C_4$−$C_5$ double bond is $\pi$-coordinated to the metal, as reflected by the Ru−$C_4$ and Ru−$C_5$ bond lengths. The Ru−$H_6$ bond is 1.579 Å, being characteristic of a single bond. The species **10** is another hydride intermediate, in which the hydride $H_6$ is cis to the Ru−$C_1$ bond. The $C_1$−$H_6$ distance in **10** is 2.008 Å. The species **11ts** is a three-centered "early" transition state from **10** to **12**, since the $C_1$−$H_6$ distance is 1.676 Å, only 0.33 Å shorter than that in **10**. In the species **12**, the two double bonds of the 1,4-diene are $\pi$-coordinated to the Ru atom.

**CpRu(H$_2$O)$^+$.** Within the ruthenacyclopentene mechanism, the calculated free energy profile of the reaction is shown in Figure 5. The geometries of all the stationary points obtained in the gas phase are given in Figure 6. Comparing the structures in Figure 6 with those in Figure 1, one can find that the species from **22** to **28** with this model catalyst are structurally similar to **2**−**8** of model I, except that $H_2O$ replaces the chloride ligand. From **28** on, however, the reaction may go along a path different from that shown in Figure 2. The hydride intermediate **28** may dissociate a $H_2O$ ligand to form the species **29** so that the $H_6$ atom can transfer to the cis site of the Ru−$C_1$ bond. This process is endothermic by about 8.9 kcal/mol. By passing the transition state **30ts** with a barrier of 1.5 kcal/mol, the species **29** converts into another hydride intermediate, **31**, in which the hydride ligand is close to the Ru−$C_1$ bond. Then, **31** undergoes a reductive elimination to produce the 1,4-diene complex **33** without a free energy barrier. The $H_2O$ ligand may recoordinate to the metal of the intermediate **33** to form the complex **34**. At last, the 1,4-diene product is detached from **34** and the catalyst is recovered. As seen from Figure 5, the highest point on the free energy profile is **23ts**, indicating that the rate-limiting step is the C−C coupling step with a free energy barrier of 11.9 kcal/mol. After the solvent effect is taken into account, the free energy of solvation for all species from **22** to **35** is about 10 kcal/mol relative to that of the reactants (**21**), but the basic feature of the free energy profile shown in Figure 5 remains unchanged. For example, the free energy barrier of the C−C coupling step in methanol is 12.5 kcal/mol, being almost identical with the value obtained in the gas phase.

According to the $\pi$-allylruthenium mechanism, the first step of the reaction would be the formation of a $\beta$-H agostic intermediate, structurally similar to species **16** except that a $H_2O$ molecule replaces the chloride ligand. In the geometry optimizations for this structure, the $H_2O$ ligand automatically dissociates from the metal center to form a $\beta$-H agostic intermediate (not shown). Thus, along the $\pi$-allylruthenium mechanism the first step should be the dissociation of the $H_2O$ ligand from the encounter complex **22**. Then, the potential energy surface of the subsequent steps should be identical with that obtained with model III ($CpRu^+$) as the catalyst, which will be described in the next subsection. A comparison between these two reaction mechanisms will also be given later.

**CpRu$^+$.** With this model catalyst, the calculated free energy profile of the ruthenacyclopentene mechanism in the gas phase or methanol is presented in Figure 7, and the corresponding structures are collected in Figure 8. According to Figure 7, the first step, the formation of the encounter complex **38**, is strongly exothermic by about 50.0 kcal/mol. Next, through a C−C coupling transition state **39ts** with a barrier of 16.5 kcal/mol the ruthenacyclopentene intermediate **40** is generated. Then, the $\beta$-H agostic intermediate **42** can be easily formed

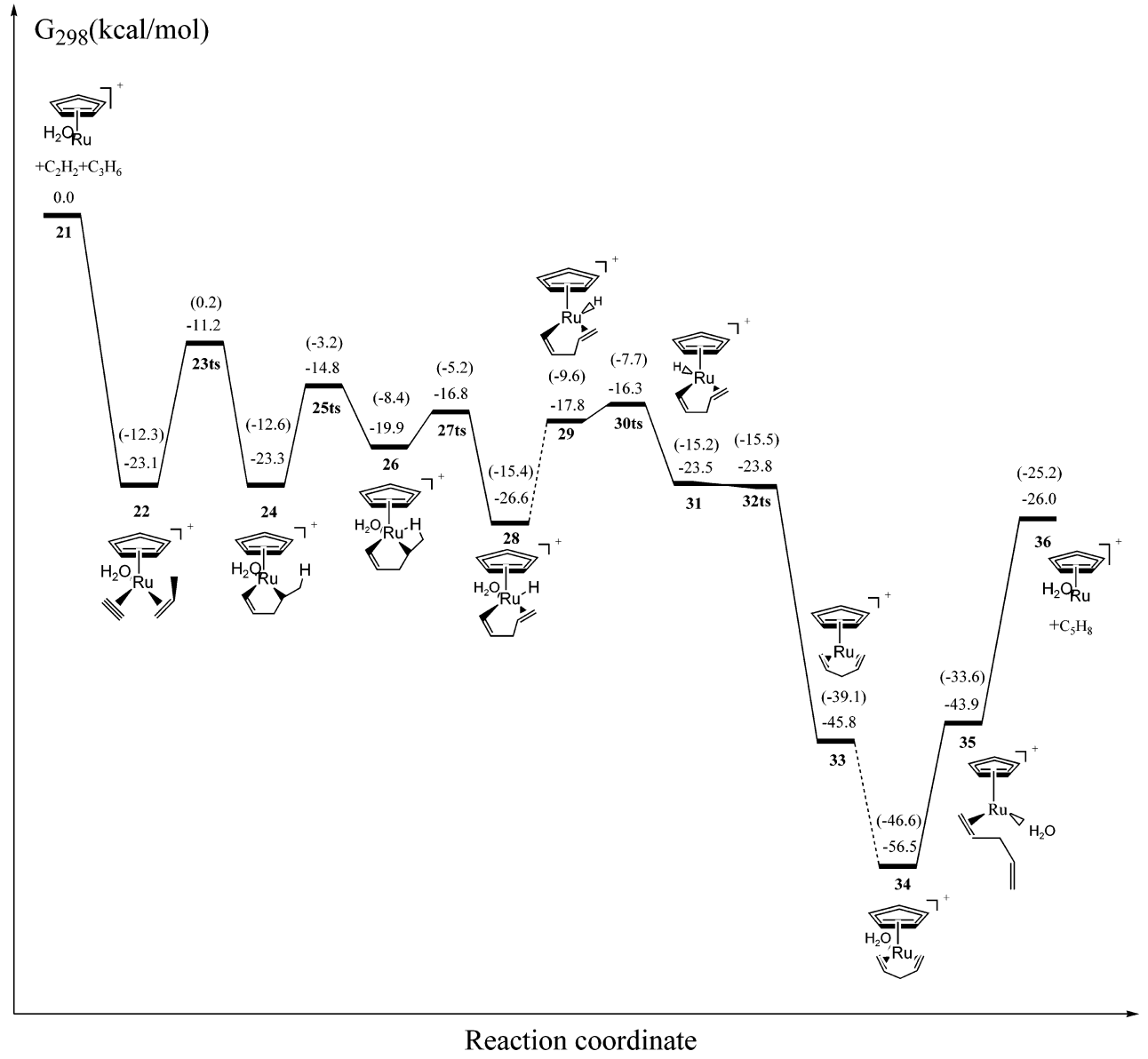


**Figure 5.** Free energy profile of the ruthenacyclopentene mechanism with model II in the gas phase and in the solution phase (values in parentheses).

via the transition state **41ts**. Through a direct hydrogen atom transfer, the species **42** can be converted to the 1,4-diene complex **44** with a very low barrier. It may be expected that a possible hydride intermediate exists between **42** and **44**. However, our calculations suggest that such a structure is not a minimum. Finally, the 1,4-diene product is removed from **44** to regenerate the model catalyst, $CpRu^+$. Comparing this dissociation step with those shown in Figures 2 and 5, one can see that, without the precoordination of the solvent molecule, the dissociation of the product from **44** is highly endothermic.

For the $\pi$-allylruthenium mechanism, the optimized geometries of all the stationary points are also collected in Figure 8. The calculated free energy profile is shown in Figure 9. One can see that, in the absence of the chloride or $H_2O$ ligand, the $\beta$-H agostic intermediate **48** can be easily generated from the encounter complex **46** via the transition state **47ts**. Then the $\beta$-H of the methyl group of the propene ligand migrates to the ethyne ligand to form the $\pi$-allylruthenium complex **50**. This process involves a free energy barrier of 9.8 kcal/mol. Although the hypothetical hydride intermediate does not exist on the potential energy surface, our intrinsic reaction coordinate (IRC) calculations show that along the reaction coordinate the $C_5-H_6$ bond is activated first and then the migration of the $H_6$ atom to the $C_1$ atom of the ethyne ligand is followed. Next, the allyl ligand and the vinyl ligand reductively couple to produce the 1,4-diene complex **44** with a barrier of 7.8 kcal/mol. This step is exothermic by about 24 kcal/mol. The last step, the loss of the product from **44**, is the same as that shown in Figure 7.

From comparison of the free energy profiles of both the ruthenacyclopentene mechanism and the $\pi$-allylruthenium mechanism, one can see that for both reaction paths the reaction is strongly exothermic at the first step but is highly endothermic at the last step. Since along both reaction pathways all other steps except the final step (the release of the product) are kinetically facile, it is hard to tell which pathway is more favorable. However, remembering that the generation of model III

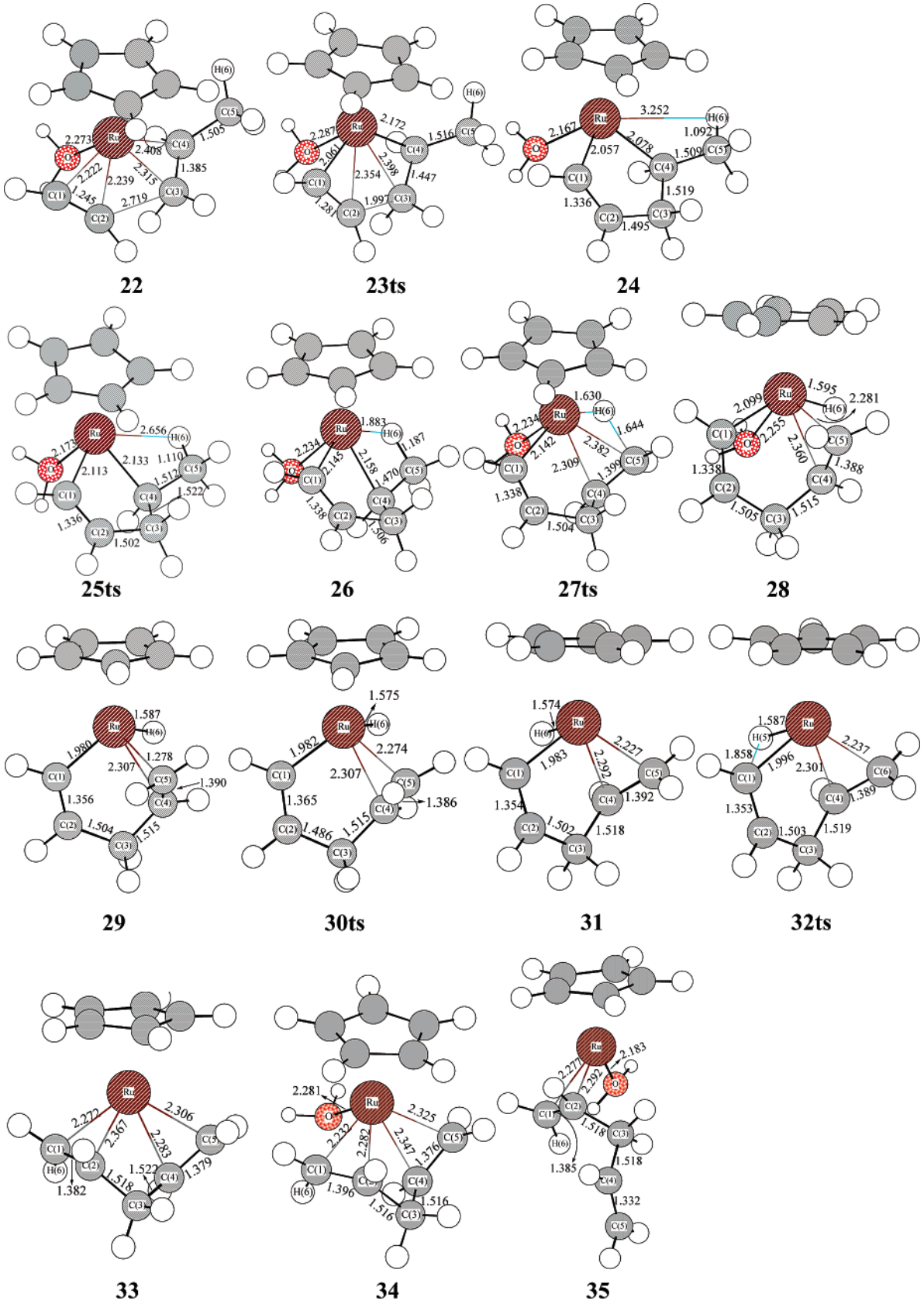


**Figure 6.** B3LYP-optimized structures of **22**−**35** in the ruthenacyclopentene mechanism obtained with model II.

from CpRuCl involves a large positive free energy change, and it is unlikely for the solvent molecule to be uncoordinated in all reaction steps, model III might be not a good candidate for the operative catalyst in related experiments.

**Comparison of Three Model Catalysts.** To gain a complete understanding on the mechanistic pathways, we have to compare the free energy profiles obtained with three model catalysts, shown in Figures 2, 3, 5, 7, and 9, respectively. The first conclusion drawn from this

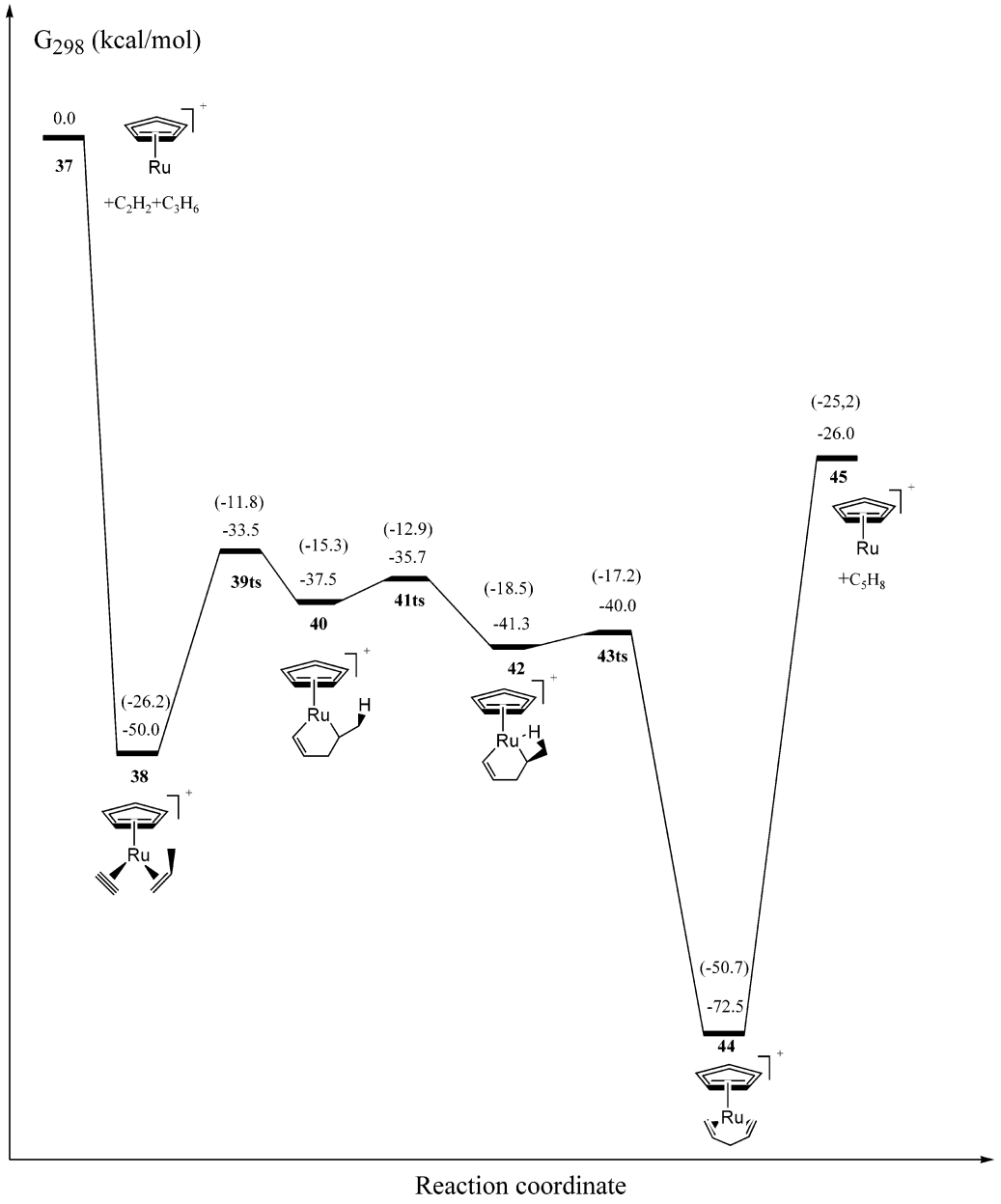


**Figure 7.** Free energy profile of the ruthenacyclopentene mechanism with model III in the gas phase and in the solution phase (values in parentheses).

comparison is that the preferred reaction pathway is solvent dependent. If the substitution reaction 1 is favored toward model I, the ruthenacyclopentene mechanism is clearly preferred over the $\pi$-allylruthenium mechanism, since the Ru−Cl bond needs to be stretched significantly in some steps on the $\pi$-allylruthenium path but does not along the ruthenacyclopentene path. According to the ruthenacyclopentene mechanism as shown in Figure 2, the overall exothermicity of the studied reaction in methanol is about 25.2 kcal/mol, and the activation free energy of the rate-determining step is 14.2 kcal/mol in solution. These results can account for the efficiency of the Alder ene reaction catalyzed by CpRu(COD)Cl in polar solvents and other experimental facts.[6] On the other hand, one can see from discussions above that model III is unlikely to be the operative catalyst.

However, considering that the calculated free energy change for the reaction 1 in methanol is only about 10.4 kcal/mol, and the accuracy of the PCM solvation energy for this reaction may be within the same order of magnitude, one cannot exclude the existence of model II. If model II is the working catalyst, we first have to combine the free energy change of the following reaction with the free energy profile shown in Figure 9 to obtain an overall picture of the $\pi$-allylruthenium pathway:

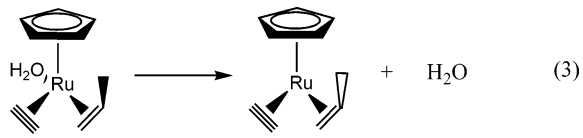


**22** **46**

The free energy change of reaction 3 is calculated to be −3.4 kcal/mol in methanol, and the corresponding electronic energy barrier is about 10.0 kcal/mol. Thus, the water dissociation from **22** to form **46** is thermodynamically and kinetically accessible at room temperature. Once the $\pi$-allylruthenium complex **50** is gener-

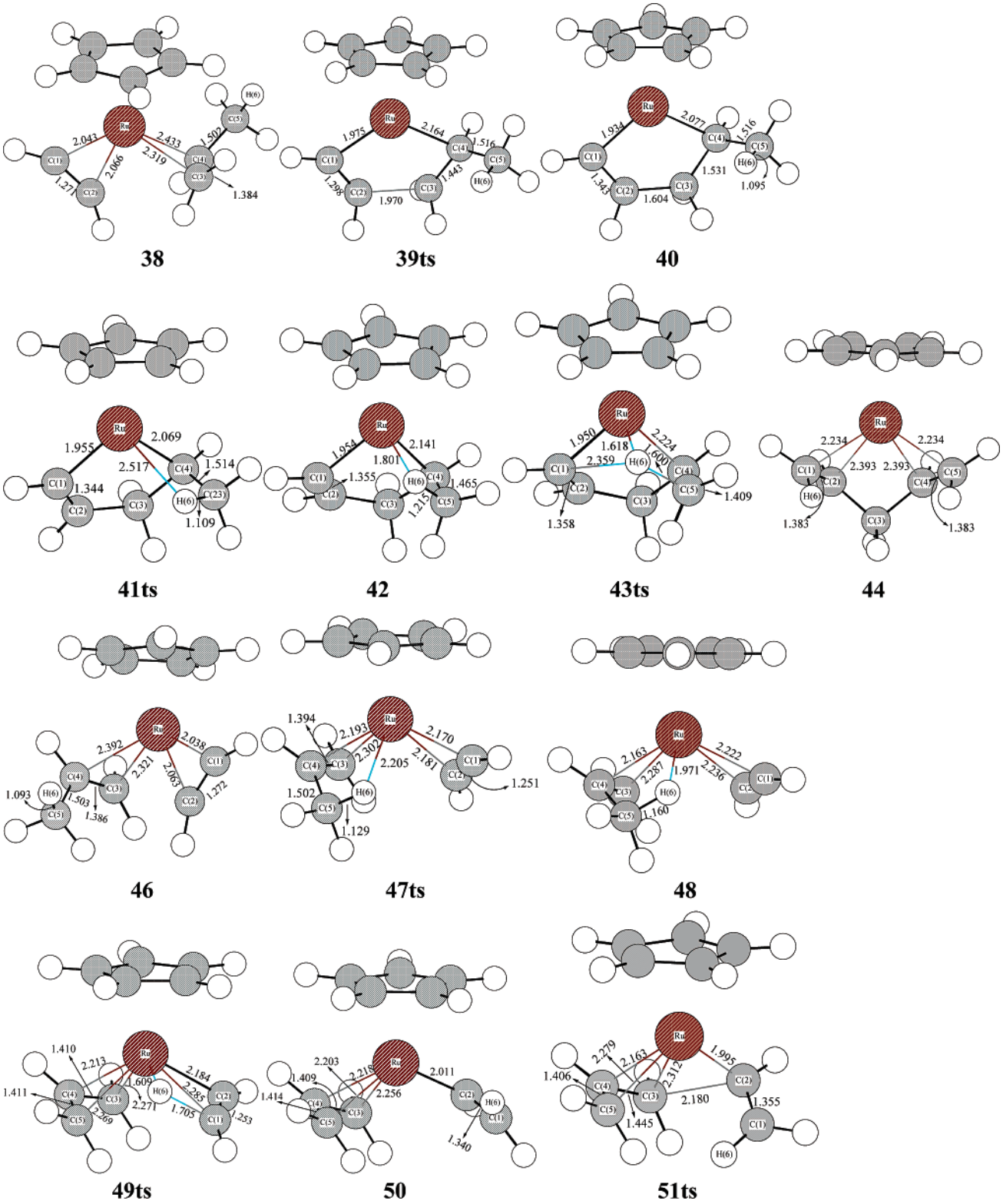


**Figure 8.** B3LYP-optimized structures of **38**−**51** obtained with model III.

ated, the water (or solvent) molecule may recoordinate to the metal center to stabilize a corresponding species such as **44**, as shown in Figure 9. Thus, the latter part of the $\pi$-allylruthenium pathway should look like the corresponding part of Figure 5. Now let us compare the energetics of two reaction mechanisms for the reaction catalyzed by model II. Assume that the free energy of **22** in methanol is taken as the energy of zero; along the ruthenacyclopentene pathway the species with the highest free energy is the C−C coupling transition state **23ts**, being 12.5 kcal/mol in solution (shown in Figure 5). Along the $\pi$-allylruthenium pathway, the species with the highest free energy is the hydrogen transfer transition state **49ts**, which is about 10.5 kcal/mol above the free energy of **22** (combining the results shown in Figure 9 and obtained for the reaction 3). Thus, when the catalyst primarily exists in the form of model II, both reaction mechanisms appear to be comparable in their

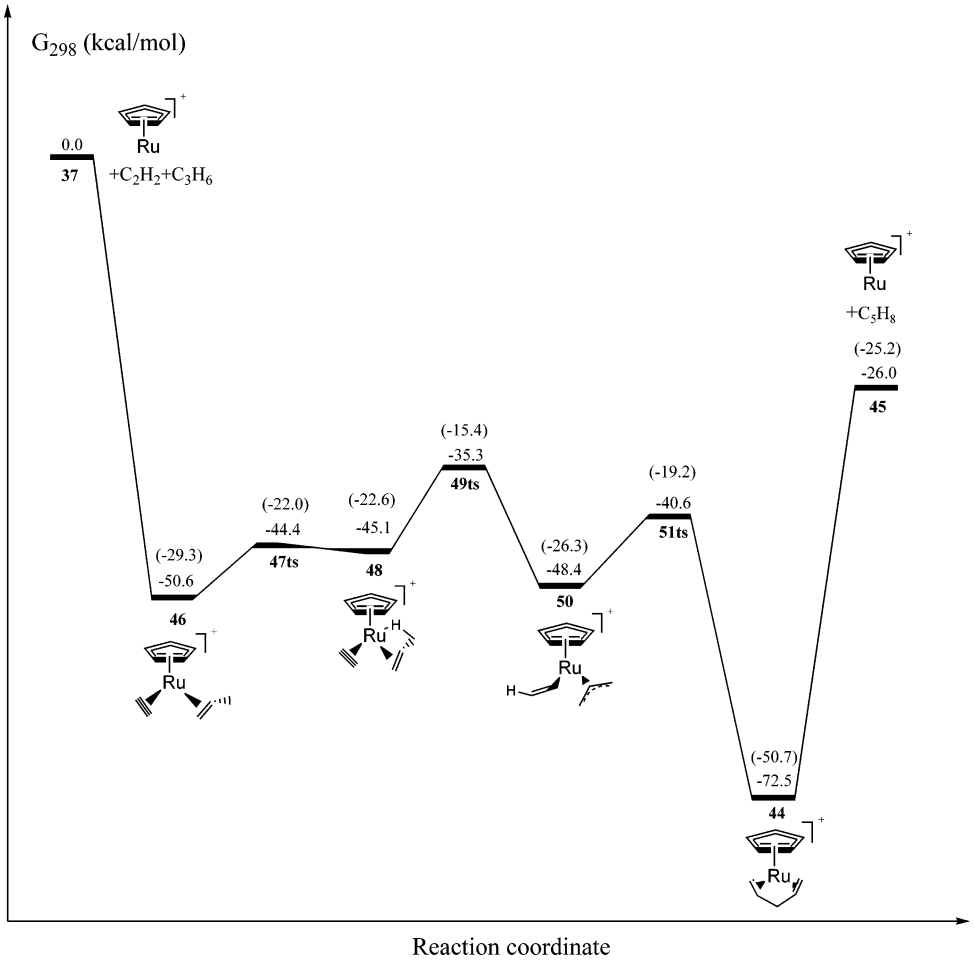


**Figure 9.** Free energy profile of the $\pi$-allylruthenium mechanism with model III in the gas phase and in the solution phase (values in parentheses).

energetics, and it is hard to distinguish between these two mechanisms from static quantum chemistry calculations reported here. In addition, one should notice that the above conclusion is drawn from calculations with a water molecule representing a coordinating solvent. If other solvent molecules are used, the mechanistic picture may be different from that which we obtained here.

## Conclusions

In this paper, we have theoretically explored the free energy profiles of the Alder ene reaction catalyzed by CpRu(COD)Cl in polar solvents. Three model catalysts, CpRuCl, $CpRuL^+$, and $CpRu^+$, have been investigated separately, and the results are compared. We have found that if CpRuCl is used as the catalyst, the ruthenacyclopentene mechanism is clearly preferred over the $\pi$-allylruthenium mechanism. The rate-determining step is the oxidative coupling of the coordinated alkyne and alkene groups to form a ruthenacyclopentene intermediate, which has a free energy barrier of 14.2 kcal/mol in the methanol solvent. The overall exothermicity of the studied reaction in methanol is about 25.2 kcal/mol. The consistency between these results and experimental facts suggests that CpRuCl may be the main form of the operative catalyst. When $CpRu^+$ is chosen as the catalyst and the solvent is assumed not to participate in the reaction, the ruthenacyclopentene mechanism and the $\pi$-allylruthenium mechanism are found to be comparable in energetics. Thus, it is difficult to distinguish between these two mechanisms by the present calculations. However, if one notices that in the absence of the chloride ligand in the coordination shell the coordinating solvent can significantly stabilize the reaction intermediates, the solvent is expected to function as a ligand, at least in some species. In the case of $CpRuL^+$, the ruthenacyclopentene intermediate can be formed readily in the presence of the coordinating solvent along the ruthenacyclopentene pathway, but the formation of the $\pi$-allylruthenium intermediate requires the solvent ligand to be removed at an earlier stage along the $\pi$-allylruthenium pathway. With $L = H_2O$, the reaction on both pathways is calculated to be thermodynamically and kinetically accessible at room temperature, but which pathway is more favorable cannot be definitely deduced from the free energy profiles of both mechanisms.

To conclude, our calculations have demonstrated that the mechanism of the Alder ene reaction catalyzed by CpRu(COD)Cl or similar compounds in polar solvents is solvent-sensitive. Since the polar solvent used noticeably affects the chemical equilibrium between CpRuCl and $CpRuL^+$ (or $CpRu^+$), the Alder ene reaction may proceed through different mechanistic pathways in different solvents.

**Acknowledgment.** Parts of the calculations were carried out on the SGI Origin 3800 computer of Nanjing University. This work was supported by the National Natural Science Foundation of China (Grant Nos. 20373022 and 20233020) and Fok Ying Tong Education Foundation (Grant No. 91014).

**Supporting Information Available:** Tables giving the computed relative energies (kcal/mol) for the stationary points of the ruthenacyclopentene mechanism with models I−III. This material is available free of charge via the Internet at http://pubs.acs.org.

OM049384I